

# Downshifting maximization procedure applied to $[\text{Eu}(\text{bphen})(\text{tta})_3]$ at different concentrations applied to a photovoltaic device and covered with a hemispherical reflector

Ricardo Guerrero-Lemus<sup>a,\*</sup>, Joaquín Sanchiz<sup>b</sup>, Marta Sierra-Ramos<sup>b</sup>, Inocencio R. Martín<sup>a</sup>, Cecilio Hernández-Rodríguez<sup>a</sup>, Dietmar Borchert<sup>c</sup>

<sup>a</sup> Departamento de Física, Instituto de Materiales y Nanotecnología (IMN), Universidad de La Laguna, Avda. Astrofísico Francisco Sánchez, 38206 La Laguna, Tenerife, Spain

<sup>b</sup> Departamento de Química, Instituto de Materiales y Nanotecnología (IMN), Universidad de La Laguna, Avda. Astrofísico Francisco Sánchez, 38206 La Laguna, Tenerife, Spain

<sup>c</sup> Fraunhofer Institute for Solar Energy Systems, Laboratory- and Servicecenter Gelsenkirchen, Auf der Reihe 2, 45884 Gelsenkirchen, Germany

## ARTICLE INFO

### Article history:

Received 9 October 2017

Received in revised form

13 December 2017

Accepted 5 January 2018

Available online 6 January 2018

### Keywords:

Solar cells

Down-shifting

Silicon

Europium

## ABSTRACT

In this work we propose the determination of the maximum downshifting efficiency of any new downshifter applied to photovoltaic (PV) devices in terms of downshifter concentration and the description of the optics applied as the standard procedure if increases in EQE, conversion efficiency and/or  $I_{sc}$  are being reported. A standard procedure is defined for determining the maximum downshifting efficiency, firstly in by reaching the solubility limit of the downshifting precursors and, subsequently, by reaching the maximum luminescent intensity of the downshifter. Also, we consider that a description of the optics applied to the experiment should be included to guarantee the reproducibility of the results. This procedure is successfully applied to poly(methylmethacrylate) (PMMA) films containing the active species  $[\text{Eu}(\text{bphen})(\text{tta})_3]$  ( $\text{bphen}$  = 4,7-biphenyl-1,10-phenanthroline and  $\text{Htta}$  = thenoltrifluoroacetone). Finally, a hemispherical reflector is applied on the PV device in order to modify the optics applied in the experimental setup and for increasing the EQE of the PV device. This scheme is proposed to be integrated in PV devices for its use in niche applications where concentrator photovoltaics (CPV) offers some advantages in relation to non-concentrator configurations.

© 2018 Elsevier B.V. All rights reserved.

## 1. Introduction

It is commonly considered that the evaluation of the downshifting properties applied to a PV device should be completed by comparing the device with the downshifting layer to a similar device with a non-luminescent layer of the same material and using the established AM1.5G spectrum [1]. However, in works where downshifters are integrated in PV devices the increase in EQE reported is not explicitly referred to a downshifter concentration where the increase in EQE reaches the maximum value [1–7] or only for some of the compounds studied [8]. In some cases (i) the studies are related to the concentration of the downshifter constituents for maximizing its photoluminescent intensity [9]; or (ii) the deposition temperature of the downshifting film for optimizing

dopant insertions and activations in the downshifter [10], but not the concentration of the downshifter itself once the best synthesis procedure and stoichiometry has been defined. In other works (i) the solubility limit is experimentally selected, but not the maximum luminescent of the downshifter [11]; (ii) the quantum dots concentration are expected to be maximized by defining a quality factor as the absorption/reabsorption coefficient, but it is difficult to obtain experimentally in comparison to the direct photoluminescent characterization of the downshifter embedded in the host material [12]; (iii) the experimental results shown are for a short set of samples in terms of downshifter concentrations and simply select the sample with the best results [13,14]; or (iv) an optimum optical density (OD) is simulated at the absorption maximum, and suggesting that increasing the absorbance would require unnecessary material consumption for a limited or no improvement in current density [15].

As it will be exposed in this work, this EQE maximum depends on the concentration of the downshifters on the PV device, but also

\* Corresponding author.

E-mail address: [rglemus@ull.edu.es](mailto:rglemus@ull.edu.es) (R. Guerrero-Lemus).

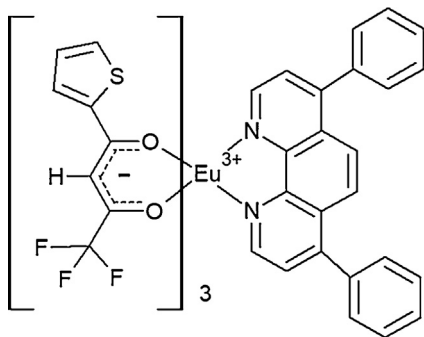


**Fig. 1.** Schematic view of the molecular structure of  $[\text{Eu}(\text{bphen})(\text{tta})_3]$ .

on the optics applied to increase the collection of photons by the solar cell. The direct relation between increase in EQE and the photoluminescent (PL) intensity of the downshifter [16] offers a simple procedure to reach the maximum increase in EQE by integrating the downshifter on the PV device. Then, we consider that previous to any EQE measurement, the downshifter concentration for reaching the maximum PL intensity should be determined.

In this work we prepare PMMA films with different ratios of the  $[\text{Eu}(\text{bphen})(\text{tta})_3]$  downshifter to determine its optimal concentration for a maximum increase in EQE for a PV mini module. Also a hemispherical reflector is placed on the downshifter-PMMA layer to avoid most photon losses due to the isotropic nature of the down-shifting emission and for increasing the EQE of a PV device placed below. This active species has been selected for absorbing UV light, helping to increase the EQE of the PV device used in this work. Moreover, downshifting in the UV range can reduce the expected yellowing of the PV module encapsulant under ambient conditions [17] and the degradation in performance for some types of solar cells (e.g. based on perovskites) [18].

## 2. Experimental

The downshifter  $[\text{Eu}(\text{bphen})(\text{tta})_3]$  active species (Fig. 1) was obtained by the reaction of stoichiometric quantities of europium (III) nitrate pentahydrate (99.99%), 4,7-biphenyl-1,10-phenanthroline (bphen, 97%), 2-thienyltrifluoroacetone (Htta, 99%), and triethylamine (99%), following a procedure similar to that previously described [19]. 2-thienyltrifluoroacetone (668 mg, 3 mmol) was dissolved in 40 ml of ethanol and the solution was heated at 65 °C under stirring in an erlenmeyer flask. Triethylamine (416 µl, 3 mmol) was added under stirring. Subsequently, a solution of bphen (332 mg, 1 mmol) in ethanol (40 ml) was added. In a different beaker,  $\text{Eu}(\text{NO}_3)_3$  (425 mg, 1 mmol) was dissolved in ethanol (10 ml). Finally, both solution were mixed and stirred for 2 h. After that time, 50 ml of water were added and a white product was obtained that was filtered, washed with water and dried in an oven at 60 °C overnight (yield 1.059 g, 92%). Elemental analysis

calculated (in %) for  $\text{C}_{48}\text{H}_{28}\text{N}_2\text{Eu}_1\text{O}_6\text{F}_9\text{S}_3$ : C, 50.23; H, 2.46; N, 2.44; S, 8.38. obtained: C, 50.47; H, 2.47; N, 2.69; S, 8.51.

PMMA films were prepared by spin coating following a procedure similar to that described previously [20]. In a typical experiment for the preparation of the films, a  $20 \times 20 \times 2$  mm bare glass is washed with a solution of soap and deionized water, dried with a dinitrogen current and placed in the holder of a spin-coater. The desired amount of sample (in our experiments in the 0.26–7.90 mg range) is dissolved in 1500 µL of  $\text{CH}_2\text{Cl}_2$  and then 26.25 mg of PMMA are added. Then, the solution is poured on the glass and spin-coated at 800 rpm for 10 s. The solvent is allowed to evaporate at room temperature. We have found that this solvent amount is enough to obtain a film that completely covers the glass and the PMMA/ $\text{CH}_2\text{Cl}_2$  ratio and spin coating conditions gives film thicknesses in the 300–470 nm range which are optimum for the EQE experiments. Finally, the glass is directly placed on a PV mini module, and illuminated for measuring the EQE (Fig. 2a). With this configuration an air gap exists between the glass and the PV device, introducing an additional optical loss. However, this configuration with an air gap has been selected because it eases placing alternative glasses on the PV mini module and, then, the EQE characterization with different downshifters. Consequently, this setup guarantees the comparison and reproducibility of results. Other authors add a refractive index matching oil carefully chosen to prevent reflection losses between the downshifter and the solar cell [15]. However, this procedure can also produce some inconveniences (e.g., poor polymer adherence to the solar cell despite the application of the matching oil) and, as our experiments are carried out only for comparative purposes, avoiding the matching oil eases the experimental procedure.

Also, a hemispherical reflector has been placed above the downshifter for collecting to the solar cell most of the downshifted photons isotropically directed out of the device (Fig. 2b). As the reflector is made of aluminum with a reflectance almost constant in the 280–1200 nm spectral range [21], no corrections to the initial EQE results have been introduced when the hemispherical reflector is used. Optimal alignment of the hemispherical reflector to the light source is needed to avoid any loss of light reaching the solar cell and, thus, obtaining the highest increase in EQE.

Luminescent spectra were obtained exciting the samples using a 400 W Xe arc lamp passed through a 0.25 m Spex 1680 double monochromator. Fluorescence was detected using a 0.25 m Spex 1681 monochromator with photomultiplier. The active specie was selected showing a large Stokes shift, avoiding overlap of emission and absorption spectra and, consequently, reemission processes in the downshifter.

The PV device is a PV mini module based on a single p-type mc-Si solar cell (non-textured and with a  $\text{SiN}_x$  antireflection coating optimized at 600 nm) encapsulated in a standard solar glass and showing a 16% conversion efficiency. A standard EQE setup based on a 100 W Xe arc lamp, double monochromator and a digital lock-in amplifier, integrated in the SPECLAB commercial setup at Fraunhofer ISE Lab (Germany) has been used. The PV mini

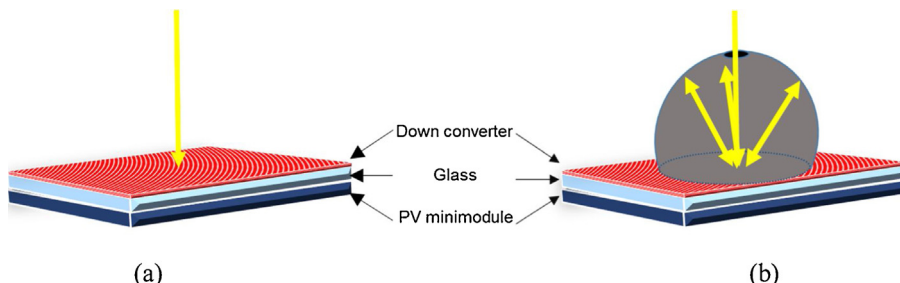


**Fig. 2.** Scheme of (a) the downshifter deposited on glass and placed on the PV mini module; and (b) the same configuration but also a hemispherical reflector placed on the downshifter for collecting to the solar cell most of the downshifted photons previously emitted isotropically out of the device.

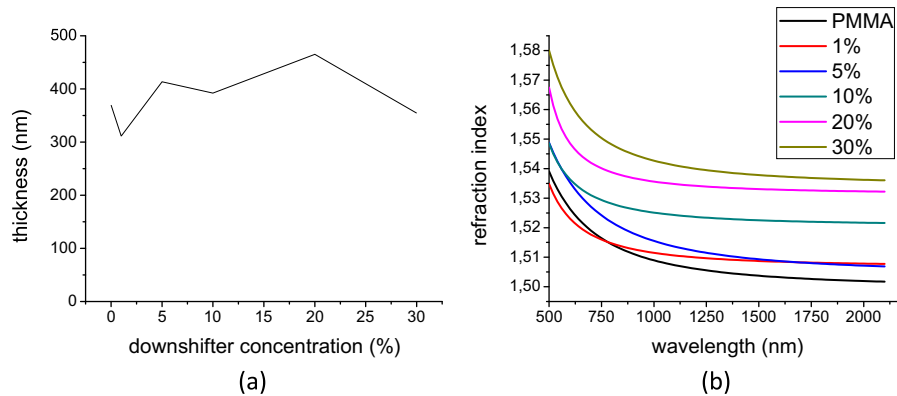


**Fig. 3.** (a) PMMA thickness and (b) refraction index of the samples with different  $[\text{Eu}(\text{bphen})(\text{tta})_3]$  concentrations.

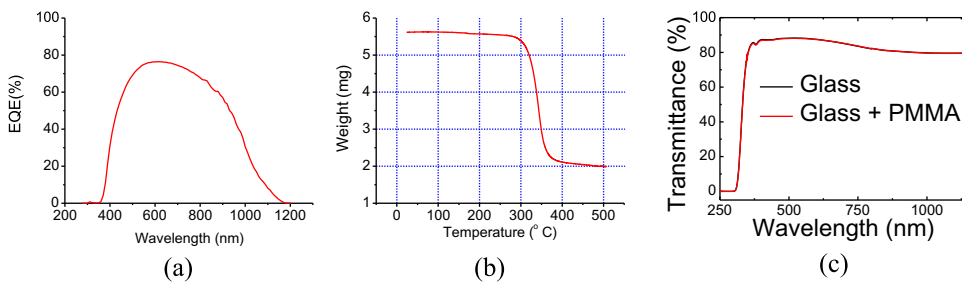


**Fig. 4.** (a) EQE of the PV mini module; (b) TG analysis of the active species; and (c) transmittance spectra of the PMMA used has host material for the active species and the glass used as substrate.

module is fixed in the EQE setup to assure the reproducibility of results between samples. Also, the glass substrates with and without the downshifter are fixed on top of the mini module when measurements with and without the hemispherical reflector are being compared. HORIBA UVISEL 2 – UV – NIR with a thickness range 1 nm–20  $\mu\text{m}$ , 190–2100 nm spectral range, minimum spot diameter 34  $\mu\text{m} \times 34 \mu\text{m}$ , 35–90° incidence, 200 × 200 mm scanning area, and prepared for measurements on textured substrates has been used to determine the thickness and refractive index of the downshifter-PMMA layer.

### 3. Results and discussion

Once the new downshifter has been selected and successfully synthesized, our proposed procedure for reaching the maximum EQE establishes that the concentration of the active species should be steeply increased to the limit of solubility. In our case the solubility limit has been reached at a  $[\text{Eu}(\text{bphen})(\text{tta})_3]/\text{PMMA}$  ratio of 30%. The results of the spectroscopic ellipsometer show that the thicknesses of the different downshifter-PMMA layers are between 311 and 465 nm (Fig. 3a), independently of the  $[\text{Eu}(\text{bphen})(\text{tta})_3]$  concentration. This small variation in thickness is attributed to an expected uncertainty of the spin-coating procedure applied for the deposition of the PMMA on the glass substrate. On the contrary, the refraction index of the PMMA layer increases up to a 2.3% when the concentration of  $[\text{Eu}(\text{bphen})(\text{tta})_3]$  embedded in PMMA increases (Fig. 3b), and attributed to the increase of the complex concentration in the PMMA film.

The PV mini module has been selected to offer almost zero EQE in the spectral range where the radiation activates the downshifting processes (280–360 nm) (Fig. 4a). The active species embedded in PMMA has been selected because it offers thermal stability up to 280  $^{\circ}\text{C}$  (Fig. 4b), does not affect the high transparency of the PMMA placed on glass (Fig. 4c), and its simple synthesis. This thermal stability limit is above the highest temperature (<160  $^{\circ}\text{C}$ ) reached

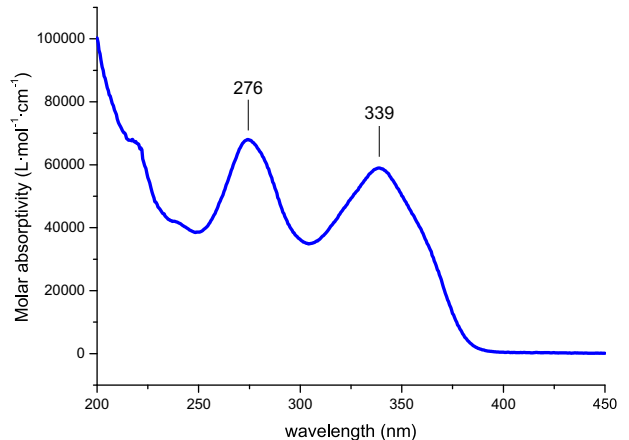


**Fig. 5.** Molar absorptivity of  $[\text{Eu}(\text{bphen})(\text{tta})_3]$  at  $5.0 \cdot 10^{-5} \text{ M}$  in  $\text{CH}_2\text{Cl}_2$ .

in the manufacturing of standard Si-based PV modules. Also it is important to mention that as the glass and PMMA substrates exhibit very close refractive indexes [22], no specific optical loss and the conservation of reflectance on the front of the system is expected to be achieved, as in this case.

This active species has also been selected for absorbing UV light, helping to reduce the expected yellowing of the PV module encapsulator under ambient conditions [17]. Thus, the active species can help to enlarge the lifetime of the mini module, as yellowing/browning is one of the more severe degradation mechanisms in these devices [23]. In this case, it is observed that the active species dissolved in a liquid solution absorbs in the UV range of the sun irradiation up to 385 nm, showing maxima at 276 and 339 nm (Fig. 5).

The absorbed photons are reemitted mainly at 615 nm (Fig. 6a) independently of the excitation wavelength in the 280–410 nm

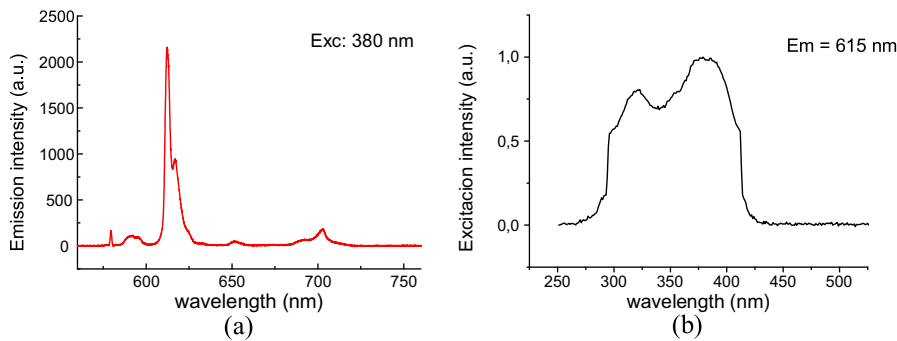


**Fig. 6.** (a) Emission spectrum of the active species embedded in PMMA and excited at 380 nm; and (b) excitation spectrum of the active species embedded in PMMA when the emission is recorded at 615 nm.

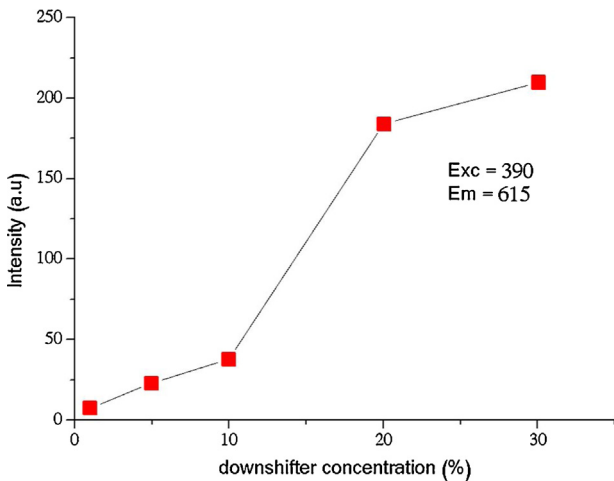


**Fig. 7.** Photoluminescent intensity at 615 nm for different downshifter concentrations embedded in PMMA and excited at 390 nm.

spectral range (Fig. 6b). The higher wavelength absorption limit is observed to be lower than the higher wavelength excitation limit. This fact can be explained in terms of the aggregation state and solvent effect produced by the PMMA in solid state and the  $\text{CH}_2\text{Cl}_2$  in the liquid solution.

Following our proposed procedure, as a first approximation for estimating the expected increase in EQE when the different  $[\text{Eu}(\text{bphen})(\text{tta})_3]$ -PMMA/glass samples were placed on the PV mini module, photoluminescent spectra of these  $[\text{Eu}(\text{bphen})(\text{tta})_3]$ -PMMA/glass samples have been obtained. A near-plateau is observed in term of emission intensity when the  $[\text{Eu}(\text{bphen})(\text{tta})_3]$  concentration reaches the solubility limit (30%) (Fig. 7).

**Table 1**

Increment in relative percent in EQE,  $I_{sc}$  and conversion efficiency for 10% and 30%  $[\text{Eu}(\text{bphen})(\text{tta})_3]$ -PMMA/glass substrate placed on the PV mini module with and without the hemispherical reflector.

	10% wo. reflector	10% w. reflector	30% wo. reflector	30% w. reflector
$\Delta \text{EQE}_{280-1200 \text{ nm}}$	+ 1.94	+ 2.40	+ 4.06	+ 6.79
$\Delta I_{sc}$	+ 1.07	+ 0.86	+ 1.92	+ 2.88
$\Delta \text{eff.}$	+ 0.17	+ 0.14	+ 0.31	+ 0.46

w.: with; wo.: without.

The EQE results are in accordance with the photoluminescent results, showing the highest increase in EQE for the downshifter with the highest photoluminescent intensity (Fig. 8a). The experimental results also show that the EQE substantially increases when the hemispherical reflector is placed on the downshifter-PMMA/glass substrate (Fig. 8b).

Increases in EQE,  $I_{sc}$  and conversion efficiency are numerically reported in Table 1 for 10% and 30%  $[\text{Eu}(\text{bphen})(\text{tta})_3]$  concentrations. The increase in short current,  $I_{sc}$ , is calculated applying the following equation [24]:

$$I_{sc} = \int_{280}^{1200} SR_{cell}(\lambda) \cdot I_r(\lambda) \cdot d\lambda \quad (1)$$

where SR is the spectral response of the PV device where  $I_r(\lambda)$  is the standard AM 1.5 reference solar spectral irradiance hemispherical on  $37^\circ$  tilted surface [25]. Estimations of the increases in PV mini module EQE, short circuit current,  $I_{sc}$ , and conversion efficiency are included in Table 1 after integrating the different EQE curves and considering that the open circuit voltage,  $V_{oc}$ , and the fill factor, FF, remain constant when the downshifter is placed on the PV mini module.

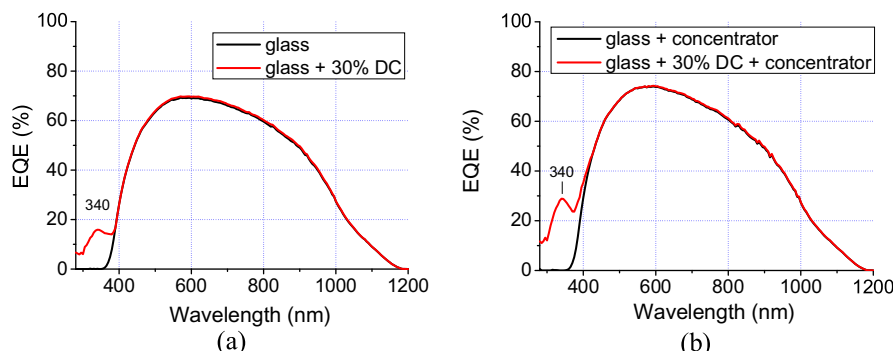


**Fig. 8.** EQE spectra for a 30%  $[\text{Eu}(\text{bphen})(\text{tta})_3]$ -PMMA/glass sample placed (a) on the PV mini module; and (b) between the hemispherical reflector and the PV mini module (as it is exposed in Fig. 2).

The EQE of the glass/PV-mini module substantially increases by placing the hemispherical reflector on the glass as the reflector redirects many photons (mostly incident photons reflected from the glass or isotropically emitted out of the device) to the PV cell. Many of these redirected photons come from edge losses of the glass where the downshifter is deposited. Thus, as the downshifters are deposited on  $20 \times 20 \times 2$  mm standard glass substrates and an air gap exists between the PV device and the glass substrate, an edge loss of about a 5% of the downshifted photons can be considered [1]. Also, about 12.5% of emitted photons from the downshifter (escape cone) escape back from the top plane of the PMMA/glass substrate (considering a refractive index of 1.5) [26,27], but most of them are redirected by the hemispherical reflector to the PV cell. This scheme with hemispherical reflector (Fig. 2b) is proposed to be integrated in PV devices for some niche applications related to concentrating photovoltaics (as in space) if a concentrating lens is placed to focus the incident light at the entrance of the reflector. This structure not only substantially increases the  $I_{sc}$  of the device and reduces the share of the PV cell in the total cost of the PV system, but also protects the solar cell from a more severe UV radiation (AM0) compared to the radiation reaching the Earth surface, thus, enlarging the durability of the PV system.

Also, it is experimentally observed that below a certain level of concentration ( $\sim 10\%$ ) the relative increase in  $I_{sc}$  (and conversion efficiency) of the PV device adding the downshifter is lower with than without the hemispherical reflector (Table 1). This is due to the fact that the hemispherical reflector also increases the  $I_{sc}$  at higher wavelengths than the spectral range (280–370 nm) where the downshifting is produced.

#### 4. Conclusions

In this work we have proposed a standard procedure for an accurate determination of the maximum downshifting efficiency of any new downshifter applied to PV devices in terms of downshifter concentration and the description of the optics applied. This kind of procedure is required if increases in EQE,  $I_{sc}$  and/or conversion efficiency are being reported and are required to be comparable with similar results reported in other works.

The standard procedure is defined for determining the maximum downshifting efficiency, firstly by reaching the solubility limit of the downshifting precursors and, subsequently, by reaching the maximum luminescent intensity of the downshifter embedded in a polymer commonly used for the encapsulation of solar cells. Also a description of the optics applied to the experiment should be included. In this work, the procedure is successfully applied to  $[Eu(bphen)(tta)_3]$ , and a direct relation between maximum photoluminescent intensity and maximum EQE, conversion efficiency and  $I_{sc}$  is validated.

Finally, a hemispherical reflector is applied to the PV device covered by the downshifter in order to modify the optics applied in the experimental setup increasing the EQE and  $I_{sc}$  of the PV device. This scheme with downshifter and hemispherical reflector is proposed to be integrated in PV devices for some niche applications related to concentrator photovoltaics.

#### Acknowledgements

This work has been supported by the Ministerio de Economía y Competitividad, Spain (Project ENE2013-41925R), co-supported by the European Social Fund. Luminescent measurements have been supported through the projects MAT2013-46649-C4-4-P, MAT2015-71070-REDC, and MAT2016-75586-C4-4-P.

#### References

- E. Klampaftis, D. Ross, K.R. McIntosh, B.S. Richards, Enhancing the performance of solar cells via luminescent down-shifting of the incident spectrum: a review, *Sol. Energy Mater. Sol. Cells* 93 (2009) 1182–1194, <http://dx.doi.org/10.1016/j.solmat.2009.02.020>.
- Y. Qin, Z. Hu, B.H. Lim, B. Yang, K.K. Chong, W.S. Chang, P. Zhang, H. Zhang, Performance improvement of dye-sensitized solar cell by introducing Sm<sup>3+</sup>/Y<sup>3+</sup> + co-doped TiO<sub>2</sub> film as an efficient blocking layer, *Thin Solid Films* 617 (2017), <http://dx.doi.org/10.1016/j.tsf.2017.03.042>.
- D. Alonso-Álvarez, D. Ross, B.S. Richards, Luminescent down-shifting for CdTe solar cells: A review of dyes and simulation of performance, *Conf. Rec. IEEE Photovolt. Spec. Conf.* (2012) 9–14, <http://dx.doi.org/10.1109/PVSC.2012.6317557>.
- A.M. Gabr, A.W. Walker, M.M. Wilkins, R. Kleiman, K. Hinzer, Procedure to decouple reflectance and down-shifting effects in luminescent down-shifting enhanced photovoltaics, *Opt. Express* 25 (2017) A530, <http://dx.doi.org/10.1364/OE.25.00A530>.
- B. McKenna, R.C. Evans, Towards efficient spectral converters through materials design for luminescent solar devices, *Adv. Mater.* 29 (2017) 1–23, <http://dx.doi.org/10.1002/adma.201606491>.
- S.D. Hodgson, W.S.M. Brooks, A.J. Clayton, G. Kartopu, D.A. Lamb, V. Barrio, S.J.C. Irvine, Increased conversion efficiency in cadmium telluride photovoltaics by luminescent downshifting with quantum dot/poly(methyl methacrylate) films, *Prog. Photovoltaics Res. Appl.* 23 (2015) 150–159, <http://dx.doi.org/10.1002/pip.2408>.
- R. Lesyuk, V. Marinov, E.K. Hobbie, A. Elbaradei, I. Tarnavchyk, Y. Bobitski, Toward cadmium-free spectral down-shifting converters for photovoltaic applications, *Sol. Energy Mater. Sol. Cells* 151 (2016) 52–59, <http://dx.doi.org/10.1016/j.solmat.2016.02.021>.
- T. Fix, A. Nonat, D. Imbert, S. Di Pietro, M. Mazzanti, A. Slaoui, L.J. Charbonnière, Enhancement of silicon solar cells by downshifting with Eu and Tb coordination complexes, *Prog. Photovoltaics Res. Appl.* 24 (2016) 1251–1260, <http://dx.doi.org/10.1002/pip.2785>.
- L. Dumont, P. Benzo, J. Cardin, I.S. Yu, C. Labbé, P. Marie, C. Dufour, G. Zatryb, A. Podhorodecki, F. Gourbilleau, Down-shifting Si-based layer for Si solar applications, *Sol. Energy Mater. Sol. Cells* (2017), <http://dx.doi.org/10.1016/j.solmat.2017.05.011>.
- K. Bouras, G. Schmerber, H. Rinnert, D. Aureau, H. Park, G. Ferblantier, S. Colis, T. Fix, C. Park, W.K. Kim, A. Dinia, A. Slaoui, Structural, optical and electrical properties of Nd-doped SnO<sub>2</sub> thin films fabricated by reactive magnetron sputtering for solar cell devices, *Sol. Energy Mater. Sol. Cells* 145 (2016) 134–141, <http://dx.doi.org/10.1016/j.solmat.2015.07.038>.
- L. Jiang, W. Chen, J. Zheng, L. Zhu, L. Mo, Z. Li, L. Hu, T. Hayat, A. Alsaedi, C. Zhang, S. Dai, Enhancing the photovoltaic performance of Perovskite solar cells with a down-conversion Eu-complex, *ACS Appl. Mater. Interfaces* 9 (2017) 26958–26964, <http://dx.doi.org/10.1021/acsami.7b10101>.
- H.J. Jeong, Y.C. Kim, S.K. Lee, Y. Jeong, J.W. Song, J.H. Yun, J.H. Jang, Ultrawide spectral response of CIGS solar cells integrated with luminescent down-shifting quantum dots, *ACS Appl. Mater. Interfaces* 9 (2017) 25404–25411, <http://dx.doi.org/10.1021/acsami.7b08122>.
- X. Hou, T. Xuan, H. Sun, X. Chen, H. Li, L. Pan, High-performance perovskite solar cells by incorporating a ZnGa2O4:Eu<sup>3+</sup>-nanophosphor in the mesoporous TiO<sub>2</sub> layer, *Sol. Energy Mater. Sol. Cells* 149 (2016) 121–127, <http://dx.doi.org/10.1016/j.solmat.2016.01.021>.
- J. Kettle, N. Bristow, D.T. Gethin, Z. Tehrani, O. Moudam, B. Li, E.A. Katz, G.A. Dos Reis Benatto, F.C. Krebs, Printable luminescent down shifter for enhancing efficiency and stability of organic photovoltaics, *Sol. Energy Mater. Sol. Cells* 144 (2016) 481–487, <http://dx.doi.org/10.1016/j.solmat.2015.09.037>.
- T. Uekert, A. Solodovnyk, S. Ponomarenko, A. Osvet, I. Levchuk, J. Gast, M. Batentschuk, K. Forberich, E. Stern, H.J. Egelhaaf, C.J. Brabec, Nanostructured organosilicon luminophores in highly efficient luminescent down-shifting layers for thin film photovoltaics, *Sol. Energy Mater. Sol. Cells* 155 (2016) 1–8, <http://dx.doi.org/10.1016/j.solmat.2016.04.019>.
- R. Rothemund, Optical modeling of the external quantum efficiency of solar cells with luminescent down-shifting layers, *Sol. Energy Mater. Sol. Cells* 120 (2014) 616–621, <http://dx.doi.org/10.1016/j.solmat.2013.10.004>.
- A.W. Czanderna, F.J. Pern, Encapsulation of PV modules using ethylene vinyl acetate copolymer as a pottant: a critical review, *Sol. Energy Mater. Sol. Cells* 43 (1996) 101–181.
- M.I. Asghar, J. Zhang, H. Wang, P.D. Lund, Device stability of perovskite solar cells – A review, *Renew. Sustain. Energy Rev.* 77 (2017) 131–146, <http://dx.doi.org/10.1016/j.rser.2017.04.003>.
- J. Zaharieva, M. Milanova, D. Todorovsky, Poly(methylmethacrylate) as immobilization matrix for europium  $\beta$ -diketonates—Morphology and fluorescent properties, *Appl. Surf. Sci.* 257 (2011) 6858–6866, <http://dx.doi.org/10.1016/j.apsusc.2011.03.019>.
- A. Le Donne, M. Acciarri, D. Narducci, S. Marchionna, S. Binetti, Encapsulating Eu<sup>3+</sup> complex doped layers to improve Si-based solar cell efficiency, *Prog. Photovoltaics Res. Appl.* 17 (2009) 519–525, <http://dx.doi.org/10.1002/pip.902>.
- Optical Reference Laboratory » Reflectance Standards, (n.d.), <http://opticalreferencelab.com/calibrated-specular-reflectance-standards/> (accessed September 26, 2017).

- [22] M.N. Polyanskiy, Refractive index database, (n.d.).  
<https://refractiveindex.info/> (accessed December 13, 2017).
- [23] T.J. Trout, W.J. Cambogi, T.C. Felder, Y. Heta, L. Garreau-Iles, K.M. Stika, PV module durability - connecting field results, accelerated testing, and materials, Washington, 45th IEEE Photovolt. Spec. Conf. (2017).
- [24] C.R. Osterwald, Calculated solar cell  $I_{SC}$  sensitivity to atmospheric conditions under direct and global irradiance, Las Vegas, NV, 18th IEEE PV Spec. Conf. IEEE (1985) 951–956.
- [25] Solar Spectral Irradiance: ASTM G-173, (n.d.).  
<http://rredc.nrel.gov/solar/spectra/am1.5/ASTMG173/ASTMG173.html> (accessed September 26, 2017).
- [26] H.J. Hovel, R.T. Hodgson, J.M. Woodall, The effect of fluorescent wavelength shifting on solar cell spectral response, Sol. Energy Mater. 2 (1979) 19–29, [http://dx.doi.org/10.1016/0165-1633\(79\)90027-3](http://dx.doi.org/10.1016/0165-1633(79)90027-3).
- [27] W. Viehmann, Thin-film scintillators for extended ultraviolet (UV) response silicon detectors, in: H.P. Field, E.F. Zalewski, F.M. Zweibaum (Eds.), International Society for Optics and Photonics, 1979, pp. 90–95, <http://dx.doi.org/10.1117/12.957960>.

## Biography

**Prof. Dr. Ricardo Guerrero-Lemus** is Doctor in Physics from Universidad Autónoma de Madrid (1996), where he served as Assistance Professor in the Department of Applied Physics between 1996 and 1999. In February 1999 he joined the Physics Department of the University of La Laguna (ULL) as Assistance Professor, Associated Professor since 2004, and Full Professor from 2016. He teaches in Renewable

Energies, Power Grids and Energy Efficiency. He is also Affiliated Research Professor of the Texas Sustainable Energy Research Institute since May 2012. Since 2006, he is the Director of the Master in Renewable Energy at the University of La Laguna. Since April 2016 he is member of the Experts Group Task-14 PVPS in the International Energy Agency (IEA). From December 2011 to June 2015 he has been appointed to the Permanent Commission of Experts in Energy of the Canary Islands Government, and from September 2016 he is board member of the Canary Islands Energy Observatory, integrated in the Canary Islands Government. He has been CEO of the Instituto Tecnológico de Canarias, Visiting Professor in the University of Texas at San Antonio in Apr–Jul 2014, May–Aug 2015 and Jul–Aug 2016, Chair in the Spanish Applied Economics Studies Foundation (FEDEA), board member of the Technological Institute for Renewable Energies (ITER, SA) of Spain, board member of the Corona del Viento SA hydro-wind power plant (El Hierro), and board member of the Güímar and Granadilla Industrial Parks. He has given countless lectures and conducted training and specialization in the area of renewable energy. His research focuses on the field of renewable energy, integration of non-dispatchable power, energy efficiency and associated technologies, having published over eighty articles in international journals, 3 books and has participated in more than thirty national and international research projects and contracts with companies (ENDESA, Enel Green Power, Abengoa, El Corte Inglés, etc.). In more than half of these projects and contracts he has served as principal investigator. He has published two books entitled “Renewable Energies and CO<sub>2</sub>. Analysis Costs, Environmental Impacts and Technological Trends”, Lecture Notes in Energy Vol. 3, Ed. Springer Verlag (2013), and “Low Carbon Energy in Africa and Latin America. Renewable Technologies, Natural Gas and Nuclear Energy”, Lecture Notes in Energy Vol. 38, Ed. Springer Verlag (2017). He is also partner in a Erasmus + funded consortia for online teaching of renewable energies in North and West African countries in the period 2017–2020.